Wind and Structures, Vol. 6, No. 1 (2003) 71-90
DOI: http://dx.doi.org/10.12989/was.2003.6.1.071

Analytical and experimental research on wind-induced vibration in high-rise buildings with tuned liquid column dampers

Ming-Yi Liu[†], Wei-Ling Chiang[‡], Chia-Ren Chu[‡] and Shih-Sheng Lin[‡†]

Department of Civil Engineering, National Central University, Taiwan, R.O.C.

(Received October 31, 2000, Revised September 30, 2002, Accepted October 22, 2002)

Abstract. In recent years, high-strength, light-weight materials have been widely used in the construction of high-rise buildings. Such structures generally have flexible, low-damping characteristics. Consequently, wind-induced oscillation greatly affects the structural safety and the comfort of the building's occupants. In this research, wind tunnel experiments were carried out to study the wind-induced vibration of a building with a tuned liquid column damper (TLCD). Then, a model for predicting the aerodynamic response in the across-wind direction was generated. Finally, a computing procedure was developed for the analytical modeling of the structural oscillation in a building with a TLCD under the wind load. The model agrees substantially with the experimental results. Therefore, it may be used to accurately calculate the structural response. Results from this investigation show that the TLCD is more advantageous for reducing the across-wind vibration than the along-wind oscillation. When the across-wind aerodynamic effects are considered, the TLCD more effectively controls the aerodynamic response. Moreover, it is also more useful in suppressing the acceleration than the displacement in biaxial directions. As s result, TLCDs are effective devices for reducing the wind-induced vibration in buildings. Parametric studies have also been conducted to evaluate the effectiveness of the TLCD in suppressing the structural oscillation. This study may help engineers to more correctly predict the aerodynamic response of high-rise buildings as well as select the most appropriate TLCDs for reducing the structural vibration under the wind load. It may also improve the understanding of wind-structure interactions and wind resistant designs for high-rise buildings.

Key words: tuned liquid column damper; aerodynamic damping ratio; wind tunnel experiment; high-rise building.

1. Introduction

In recent years, high-strength, light-weight materials have been widely used in the construction of high-rise buildings. Such structures generally have flexible, low-damping characteristics. Because of these wind sensitive properties, building vibration under the wind load has become a research area of great interest. Wind-induced structural displacement affects the structural safety and acceleration greatly influences the comfort of the building's occupants. However, these phenomena involve complex aerodynamic effects, especially in the across-wind direction. Consequently, it is of

† Ph. D
‡ Professor
‡† Master

particular importance to search for effective and practical devices which will be capable of suppressing the structural vibration induced by the wind load.

High-rise buildings oscillate in both the along-wind and the across-wind directions. Along-wind motion is primarily a result of pressure differences on the windward and the leeward faces, which is generally influenced by turbulent fluctuations in the approaching flow. The aerodynamic effects can therefore be neglected. In addition, the along-wind response can be quantified analytically by utilizing quasi-steady and strip theories (Kareem 1992). Across-wind motion is induced by the periodic vortex shedding from both sides of a building. Accordingly, the aerodynamic effects are very complicated. Many wind tunnel experiments have been carried out to examine this wind-structure interaction (Kwok 1982, Kareem 1984, Matsumoto 1986 and Kawai 1992). However, no suitable theory for calculating this complex across-wind aerodynamic response has been formulated.

The tuned liquid column damper (TLCD) was first proposed by Sakai, *et al*. (1989), consisting of a U-tube container with an orifice in the middle. It dissipated the energy of structural oscillation by the combined action of inertia force caused by the movement of the liquid, the restoring load induced by gravity acting on the liquid and the damping effect caused by an orifice. Xu, *et al*. (1992a and 1992b) studied the effectiveness of a TLCD in controlling the wind-induced vibration of a tall building. They analyzed a typical structure modeled as a multi-degree-of-freedom oscillation system. The along-wind turbulence and the across-wind wake excitation were simulated both as stationary and stochastic processes. Samali, *et al*. (1992) performed parametric studies of a TLCD that included the mass ratio, the tuning ratio and the orifice opening ratio, revealing that a TLCD could provide enough vibration suppression capacity for a forty-story building subjected to the stationary seismic load. Sun, *et al*. (1993) have proposed a mathematical model of the wind-induced stochastic response of a building with a TLCD in the along-wind direction. This investigation showed that a TLCD would have significant advantages if the parameters were selected properly. Balendra, *et al*. (1995) have suggested that the effectiveness of a TLCD was dependent on the structural damper and the excitation characteristics. Optimally, the tuning ratio should be 1.0 and the orifice opening ratio should be between 0.5 and 1.0. Won, *et al*. (1997) used random vibration theory to evaluate the performance of a flexible building with a TLCD under the random seismic load. The earthquake motion was simulated as a non-stationary stochastic process with both frequency and amplitude modulations. Gao and Kwok (1997) proved that the TLCD was equally effective for harmonic excitation as well as stationary random excitation. They also indicated that the optimal tuning ratio would be independent of the excitation. As indicated earlier, many theoretical models for predicting the effectiveness of the TLCD have been developed. However, there have been few experiments in support of these models.

As mentioned above, no proper theory has been formulated for evaluating the aerodynamic response in the across-wind direction. Furthermore, few experiments have verified the vibration suppression performance of the TLCD. In this research, therefore, wind tunnel experiments were carried out to study the wind-induced oscillation of a building with a TLCD. Then, a model for predicting the aerodynamic response in the across-wind direction was generated. A computing procedure was also developed for the analytical modeling of the structural response in a building with a TLCD under the wind load. The accuracy of this model can be proven experimentally. Parametric studies were also used to calculate the effectiveness of the TLCD in controlling the wind-induced vibration in a structure. This study may help engineers to more correctly predict the aerodynamic response of high-rise buildings. In addition, they could select the most appropriate TLCDs for reducing the structural oscillation due to the wind load, which lead to an improved

understanding of wind-structure interactions and wind resistant designs for high-rise buildings.

2. Mathematical model

In this chapter, a predictive model of across-wind aerodynamic response is described. A computing procedure for analytically modeling the wind-induced vibration in a building with a TLCD in both the along-wind and the across-wind directions has also been created in this study.

2.1. Equation of motion

A high-rise building with a TLCD can be simulated as a two-degree-of-freedom oscillation system, as shown in Fig. 1. M_1, C_1 and K_1 are the mass, the damping coefficient and the stiffness of the building, respectively. H_2 and B_2 represent the vertical height and the horizontal breadth of the TLCD. Its total length is L_2 ($=B_2+2H_2$) and its dimensional ratio is λ ($\equiv B_2/L_2$). ρ_1 is the liquid density and β is the head loss coefficient. Balendra, *et al.* (1995) have indicated that β is correlated with the orifice opening ratio κ ($\equiv A_o/A_h$, see Fig. 1). $F(t)$ is the time history of the along-wind and across-wind loads, respectively. X_1 and X_2 are the displacement of the building and the TLCD. The TLCD's vertical and horizontal cross-sectional areas are defined as A_v and A_h, respectively. The area ratio is χ ($\equiv A_v/A_h$). The equation of motion can be generated by Lagrange's equation, that is;

$$\begin{bmatrix} M_1 + \rho_1 A_v(2H_2 + B_2/\chi) & \rho_1 A_v B_2 \\ \rho_1 A_v B_2 & \rho_1 A_v(2H_2 + \chi B_2) \end{bmatrix} \begin{Bmatrix} \ddot{X}_1 \\ \ddot{X}_2 \end{Bmatrix} + \begin{bmatrix} C_1 & 0 \\ 0 & \frac{1}{2}\rho_1 A_v \chi \beta |\dot{X}_2| \end{bmatrix} \begin{Bmatrix} \dot{X}_1 \\ \dot{X}_2 \end{Bmatrix} + \begin{bmatrix} K_1 & 0 \\ 0 & 2\rho_1 A_v g \end{bmatrix} \begin{Bmatrix} X_1 \\ X_2 \end{Bmatrix} = \begin{Bmatrix} F(t) \\ 0 \end{Bmatrix} \tag{1}$$

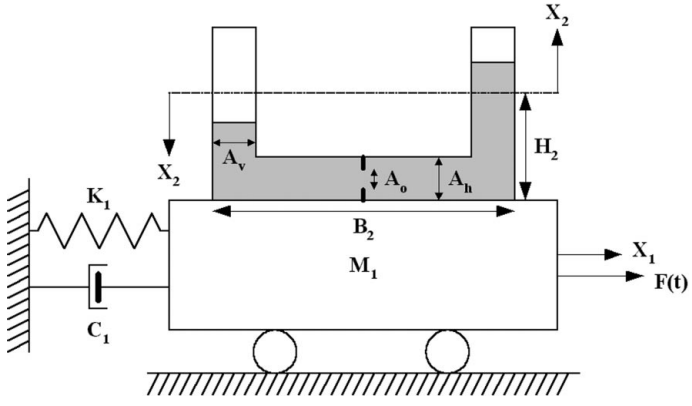

Fig. 1 Two-degree-of-freedom oscillation system

Xu, *et al*. (1992a and 1992b) have demonstrated that $\dot{X}_2$ is a zero-mean stationary Gaussian process. Then, the equivalent linearized damping coefficient of the TLCD C_2 can be evaluated by using the equivalent linearization method (Iwan and Yang 1972), so that;

$$C_2 = \sqrt{\frac{2}{\pi}}\rho_1 A_v \chi \beta \sigma_{\dot{X}_2} \tag{2}$$

where $\sigma_{\dot{X}_2}$ is the root-mean-square (RMS) velocity of the TLCD. Since C_2 depends on $\sigma_{\dot{X}_2}$, an iteration solution procedure is generally required to calculate this equation. Eq. (1) can be rewritten by substituting Eq. (2) into Eq. (1), that is;

$$\begin{bmatrix} M_1 + M_2 & M_4 \\ M_4 & M_3 \end{bmatrix} \begin{Bmatrix} \ddot{X}_1 \\ \ddot{X}_2 \end{Bmatrix} + \begin{bmatrix} C_1 & 0 \\ 0 & C_2 \end{bmatrix} \begin{Bmatrix} \dot{X}_1 \\ \dot{X}_2 \end{Bmatrix} + \begin{bmatrix} K_1 & 0 \\ 0 & K_2 \end{bmatrix} \begin{Bmatrix} X_1 \\ X_2 \end{Bmatrix} = \begin{Bmatrix} F(t) \\ 0 \end{Bmatrix} \tag{3a}$$

where;

$$M_2 = \rho_1 A_v (2H_2 + B_2/\chi) \tag{3b}$$

$$M_3 = \rho_1 A_v (2H_2 + \chi B_2) \tag{3c}$$

$$M_4 = \rho_1 A_v B_2 \tag{3d}$$

$$K_2 = 2\rho_1 A_v g \tag{3e}$$

The mass ratio and the tuning ratio for this oscillation system are μ ($\equiv M_2/M_1$) and δ ($\equiv \omega_2/\omega_1$), respectively, where ω_1 and ω_2 are the natural circular frequency of the structure and the TLCD, separately.

Supposing that the wind load has the exponential form $F(t)=e^{i\omega t}$, then the transfer functions with complex forms can be computed by utilizing Fourier transform in Eq. (3a), so that;

$$H_{X_1}(\omega) = \frac{-\omega^2 M_3 + i\omega C_2 + K_2}{\Delta} \tag{4a}$$

$$H_{\ddot{X}_1}(\omega) = \frac{\omega^4 M_3 - i\omega^3 C_2 - \omega^2 K_2}{\Delta} \tag{4b}$$

$$H_{X_2}(\omega) = \frac{\omega^2 M_4}{\Delta} \tag{4c}$$

$$H_{\ddot{X}_2}(\omega) = \frac{-\omega^4 M_4}{\Delta} \tag{4d}$$

$$\begin{aligned} \Delta = {} & \omega^4[M_3(M_1 + M_2) - M_4^2] - i\omega^3[M_3 C_1 + C_2(M_1 + M_2)] \\ & -\omega^2[M_3 K_1 + C_1 C_2 + K_2(M_1 + M_2)] + i\omega(C_2 K_1 + C_1 K_2) + K_1 K_2 \end{aligned} \tag{4e}$$

where $H_{X_1}(\omega)$, $H_{\ddot{X}_1}(\omega)$, $H_{X_2}(\omega)$ and $H_{\ddot{X}_2}(\omega)$ are the transfer functions of the displacement and the acceleration of the building and the TLCD, respectively.

2.2. Aerodynamic damping ratio

Aerodynamic effects are slight in the along-wind direction, whereas they are complicated in the across-wind direction. Consequently, only the across-wind direction effects were considered in this study. The aerodynamic damping ratio ξ_a is generally used to determine these complex phenomena. ξ_a is correlated with many influential parameters, but there is no proper theory to evaluate it. Many wind tunnel experiments have been carried out to estimate ξ_a. However, only partial parameters have been considered in these experimental studies. These investigations may not be complete lacking generality. In order to improve this situation, we originated a predictive model of ξ_a which combines six significant parameters.

Vickery (1981) has demonstrated that ξ_a is inversely proportional to Scruton number S_c, that is;

$$\xi_a = C_1 \frac{1}{S_c} \tag{5a}$$

where C_1 is a constant. Vickery and Basu (1983) have indicated an empirical formula whereby ξ_a can be expressed as the polynomial function of the turbulent intensity T_i, such that;

$$\xi_a = C_2(19.6T_i^4 - 37.3T_i^3 + 24.8T_i^2 - 7.1T_i + 1.0) \tag{5b}$$

where C_2 is a constant. $\sigma^o_{X_{1y}}$ is the dimensionless RMS displacement of the structure in the across-wind direction. The research of Basu and Vickery (1983) has revealed that ξ_a is dependent on the square of $\sigma^o_{X_{1y}}$, so that;

$$\xi_a = C_3 \sigma^{o\ 2}_{X_{1y}} \tag{5c}$$

where C_3 is a constant. Vickery and Basu (1984) have suggested that ξ_a can be presented as the logarithmic function of the aspect ratio A_r, that is;

$$\xi_a = C_4(0.4 \ln A_r - 0.1) \tag{5d}$$

where C_4 is a constant. The reduced wind velocity $\overline{U}_r$ and the reduced resonant wind velocity $\overline{U}_r^L$ (defined as $\overline{U}_r$ when the lock-in phenomenon occurs) are both dimensionless parameters. Cheng, *et al*. (1999) have performed experimental studies to obtain an exponential formula for ξ_a correlated with $\overline{U}_r$ and $\overline{U}_r^L$, that is;

$$\xi_a = C_5 \exp[C_6(\overline{U}_r - \overline{U}_r^L)^2] \tag{5e}$$

where C_5 and C_6 are constants. From the above description, ξ_a is a function of S_c, T_i, $\sigma^o_{X_{1y}}$, A_r, $\overline{U}_r$ and $\overline{U}_r^L$, respectively. A predictive model of ξ_a in the across-wind direction can be generated by

combining Eq. (5a) to Eq. (5e) as follows;

$$\xi_a = C_1^* \frac{\sigma_{X_{1y}}^{o\ 2}}{S_c} \exp[C_2^*(\overline{U}_r - \overline{U}_r^L)^2](0.4\ln A_r - 0.1)(19.6T_i^4 - 37.3T_i^3 + 24.8T_i^2 - 7.1T_i + 1.0) \quad (5f)$$

where C_1^* and C_2^* are undetermined coefficients. Based on the series of wind tunnel experiments discussed in chapter three, these two coefficients can be determined. In engineering applications, Eq. (5f) may be sufficiently employed if the aims it is intended to serve are modest. Then, the aerodynamic damping coefficient C_a can be presented, such that;

$$C_a = 2\xi_a\sqrt{M_1 K_1} \quad (6)$$

Eq. (3a) can be modified by Eq. (6), that is;

$$\begin{bmatrix} M_1 + M_2 & M_4 \\ M_4 & M_3 \end{bmatrix} \begin{Bmatrix} \ddot{X}_1 \\ \ddot{X}_2 \end{Bmatrix} + \begin{bmatrix} C_1 + C_a & 0 \\ 0 & C_2 \end{bmatrix} \begin{Bmatrix} \dot{X}_1 \\ \dot{X}_2 \end{Bmatrix} + \begin{bmatrix} K_1 & 0 \\ 0 & K_2 \end{bmatrix} \begin{Bmatrix} X_1 \\ X_2 \end{Bmatrix} = \begin{Bmatrix} F(t) \\ 0 \end{Bmatrix} \quad (7)$$

Eq. (7) is the equation of motion showing the aerodynamic response of a high-rise building with a TLCD in the across-wind direction. The along-wind response can also be calculated utilizing the same equation but without C_a.

2.3. Wind load

Fig. 2 illustrates the wind load on a high-rise building. The wind load can be decomposed into an

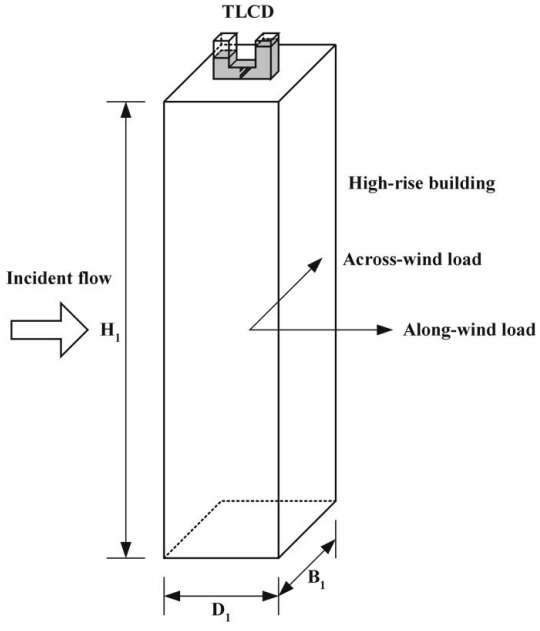

Fig. 2 Wind load on a high-rise building

average and a fluctuating component. Only the fluctuating load is considered in this wind load model.

Davenport's along-wind load spectrum $S_{F_{ij_x}}(\omega)$ (Davenport 1976) is utilized in this research. A one-sided cross spectrum of the wind load on the i-th and the j-th floors can be expressed as follows;

$$S_{F_{ij_x}}(\omega) = \frac{8\bar{F}_{i_x}\bar{F}_{j_x}K_0\bar{U}_{10}^2}{\bar{U}_i\bar{U}_j\omega}\frac{(600\omega/\pi\bar{U}_{10})^2}{[1+(600\omega/\pi\bar{U}_{10})^2]^{4/3}}\exp\left[-\frac{C_x\omega}{\pi}\frac{|z_i-z_j|}{(\bar{U}_i+\bar{U}_j)}\right] \tag{8a}$$

where z_i is the height of the i-th floor, $\bar{U}_i$ is the mean wind velocity on the i-th floor, $\bar{F}_{i_x}$ is the mean wind load of the i-th floor in the along-wind direction, $\bar{U}_{10}$ is the reference mean wind velocity 10 m above the ground (m/sec), K_0 is the roughness coefficient which depends on surface roughness of the ground and C_x is the decay coefficient in the along-wind direction. The exponential term in Eq. (8a) is the coherence function for the i-th and the j-th floors. Furthermore, $\bar{U}_i$ is assumed to follow the power law distribution, that is;

$$\frac{\bar{U}_i}{\bar{U}_{10}} = \left(\frac{z_i}{10}\right)^{\alpha} \tag{8b}$$

where α is the power law exponent. Since the aerodynamic effects are slight in the along-wind direction, $\bar{F}_{i_x}$ can be individually calculated by $\bar{U}_i$, such that;

$$\bar{F}_{i_x} = 0.5\rho_a\bar{U}_i^2A_i\overline{C_d} \tag{8c}$$

where ρ_a is the air density, A_i is the area of the windward side and $\overline{C_d}$ is the mean drag coefficient.

Ohkuma and Kanaya's across-wind load spectrum $S_{F_{ij_y}}(\omega)$ (Ohkuma and Kanaya 1978) is utilized in this study. Because the aerodynamic effects are complicated in the across-wind direction, the wind load cannot be directly evaluated by the wind velocity. Ohkuma and Kanaya have used aerodynamic coefficients to experimentally generate $S_{F_{ij_y}}(\omega)$. A one-sided cross spectrum of the wind load on the i-th and the j-th floors can be presented as follows;

$$S_{F_{ij_y}}(\omega) = \frac{8B_w\sigma_{F_{iy}}\sigma_{F_{jy}}}{\omega}\frac{(\eta_i\eta_j/S_t^2)}{[1-(\eta_i\eta_j/S_t^2)]^2+4B_w^2(\eta_i\eta_j/S_t^2)}\exp\left[-\frac{C_y\omega}{\pi}\frac{|z_i-z_j|}{(\bar{U}_i+\bar{U}_j)}\right] \tag{9a}$$

where;

$$\eta_i = \frac{\omega B_i}{2\pi\bar{U}_i} \tag{9b}$$

$$S_t = 0.135 - 0.069\exp(-0.056A_r) \tag{9c}$$

$$B_w = 0.6\exp(-0.3A_r) \tag{9d}$$

and where η_i is a dimensionless parameter of the i-th floor, B_i is the structural dimension of the

windward side on the i-th floor, $\sigma_{F_{i_y}}$ is the RMS wind load of the i-th floor in the across-wind direction, S_t is the Strouhal number, B_w is the bandwidth coefficient and C_y is the decay coefficient in the across-wind direction. The exponential term in Eq. (9a) is the coherence function for the i-th and the j-th floors. Moreover, in engineering applications, S_t can be calculated by Eq. (9c).

Assuming that the mode shape of the vibration system is linear. Then, the generalized Davenport's along-wind load spectrum $\bar{S}_{F_{11_x}}(\omega)$ and Ohkuma and Kanaya's across-wind load spectrum $\bar{S}_{F_{11_y}}(\omega)$ can be evaluated, respectively, that is;

$$\bar{S}_{F_{11_x}}(\omega) = \int_0^{H_1}\int_0^{H_1} S_{F_{ij_x}}(\omega)\phi(z_i)\phi(z_j)dz_i dz_j \tag{10a}$$

$$\bar{S}_{F_{11_y}}(\omega) = \int_0^{H_1}\int_0^{H_1} S_{F_{ij_y}}(\omega)\phi(z_i)\phi(z_j)dz_i dz_j \tag{10b}$$

where $\phi(z_i)$ $\left(\equiv \dfrac{z_i}{H_1}\right)$ is the mode shape value of z_i and H_1 is the height of the building, separately.

2.4. Structural response

In this research, a high-rise building with a TLCD is considered as a two-degree-of-freedom oscillation system. The RMS response of the structure can be calculated by combining and integrating the transfer function (Eq. (4a) and Eq. (4b)) and the generalized wind load spectrum (Eq. (10a) and Eq. (10b)) individually into the frequency domain, such that;

$$\sigma_{X_{1_x}} = \sqrt{\int_{-\infty}^{\infty} \left|H_{X_1}(\omega)\right|^2 \bar{S}_{F_{11_x}}(\omega)d\omega} \tag{11a}$$

$$\sigma_{X_{1_y}} = \sqrt{\int_{-\infty}^{\infty} \left|H_{X_1}(\omega)\right|^2 \bar{S}_{F_{11_y}}(\omega)d\omega} \tag{11b}$$

$$\sigma_{\ddot{X}_{1_x}} = \sqrt{\int_{-\infty}^{\infty} \left|H_{\ddot{X}_1}(\omega)\right|^2 \bar{S}_{F_{11_x}}(\omega)d\omega} \tag{11c}$$

$$\sigma_{\ddot{X}_{1_y}} = \sqrt{\int_{-\infty}^{\infty} \left|H_{\ddot{X}_1}(\omega)\right|^2 \bar{S}_{F_{11_y}}(\omega)d\omega} \tag{11d}$$

where $\sigma_{X_{1_x}}$, $\sigma_{X_{1_y}}$, $\sigma_{\ddot{X}_{1_x}}$ and $\sigma_{\ddot{X}_{1_y}}$ are the RMS displacement and the RMS acceleration of the building in the along-wind and the across-wind directions, respectively.

With the above description, a computing procedure of an analytical model was generated and is shown in Fig. 3. This model can evaluate the wind-induced vibration of a high-rise building with a TLCD in both the along-wind (without ξ_a) and the across-wind (with ξ_a) directions. In addition, the accuracy of this predictive model was verified by the wind tunnel experiments described in chapter three.

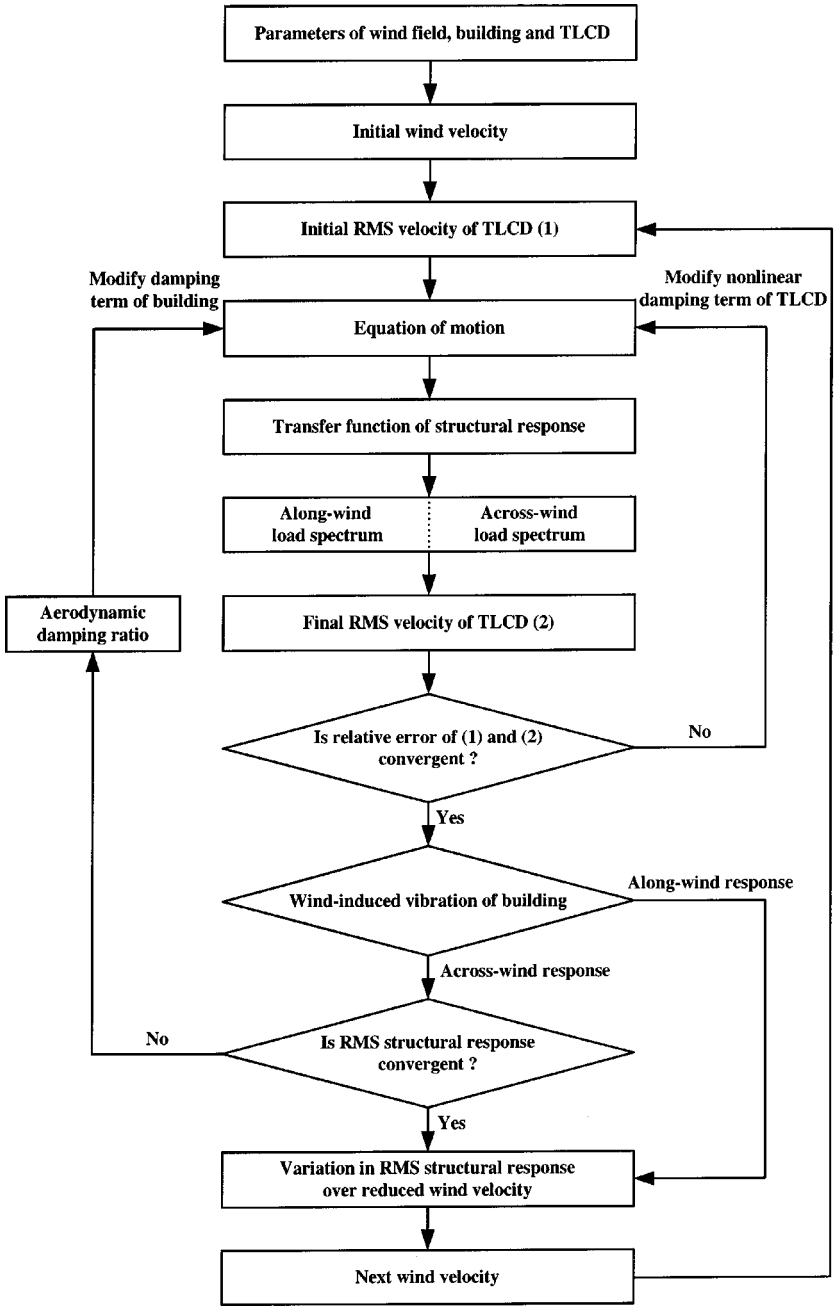

Fig. 3 Computing procedure of analytical model for structural vibration with TLCD under wind load

3. Experimental investigations

A series of wind tunnel experiments were carried out to study the wind-induced vibration of a building with a TLCD. Two undetermined coefficients were then obtained for the model to predict

the aerodynamic damping ratio. Furthermore, a procedure for computing the analytical modeling of the structural response in a building with a TLCD under the wind load was verified experimentally.

3.1 Wind tunnel model

The experiments were carried out in a wind tunnel (located at National Central University) with a working section of 3.0 m × 2.1 m and 30.0 m long. A 1:200 scale model of a building (0.2 m × 0.1 m × 0.75 m) with a rigid wooden construction was used. The aspect ratio A_r was 5.3. Five wind load components (the drag force, the side force, the rolling moment, the pitching moment and the yawing moment) were measured by a high-frequency force balance, shown in Fig. 4(a). Fig. 4(b) illustrates the instrument for measuring structural vibration. The model could pivot at the base by a gimbal arrangement. It was restrained by two pairs of springs. A circular plate immersed in oil simulated the viscous damping of the structure. The TLCDs were made of acrylic plates. Glycerin was added to these U-tube containers. The mass ratio μ was the variable in this experimental investigation. The building's and the TLCDs' parameters are shown in Table 1, Table 2(a) and Table 2(b), respectively. The breadth (B_1) and the depth (D_1) are the dimensions of the building, perpendicular and parallel to the incident flow, separately. In this research, $D_1/B_1 = 2.0$ and 0.5 were studied, as shown in Fig. 5. It reveals that the yawing angle is 0^o and 90^o, respectively. Fig. 4(b) also indicates two laser displacement sensors and one accelerometer that were installed to measure

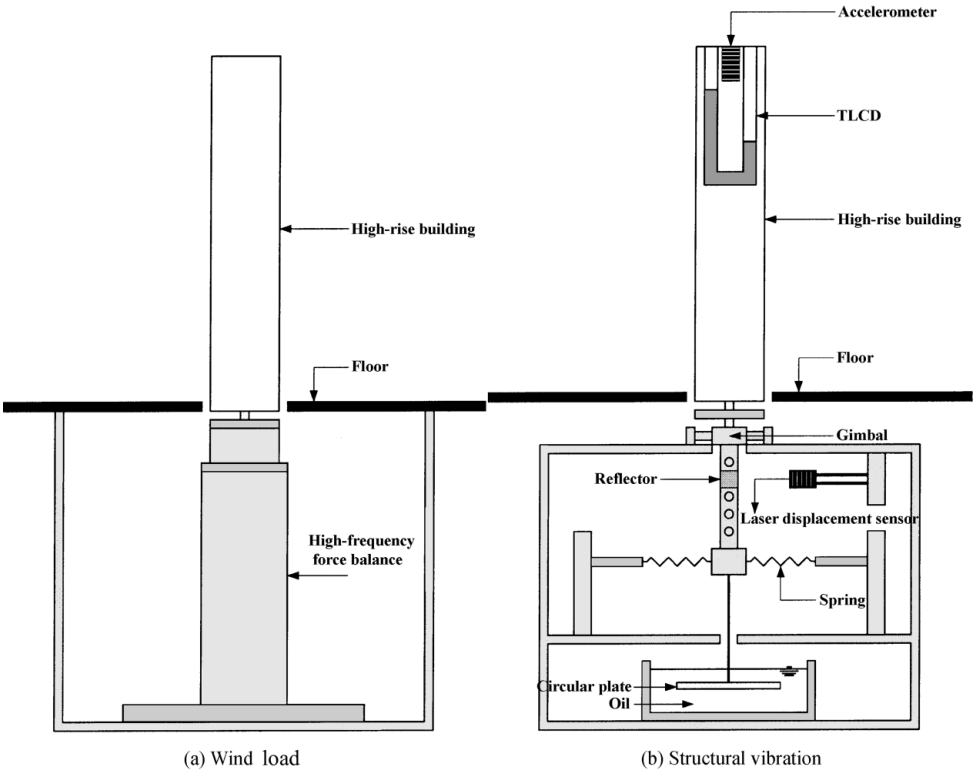

Fig. 4 Measurement instruments in experiments

Table 1 The building's parameters in experiments

Mass M_1(kg)	Damping coefficient C_1(N-sec/m)	Stiffness K_1(N/m)	Natural circular frequency ω_1(rad/sec)	Damping ratio ξ_1
1.28	1.60	1258.38	31.42	0.02

Table 2 (a) TLCDs' invariable parameters in experiments

Vertical height H_2(m)	Horizontal breadth B_2(m)	Liquid density ρ_1(kg/m^3)	Head loss coefficient β	Tuning ratio δ	Dimensional ratio λ	Orifice opening ratio κ	Area ratio χ
0.03	0.11	1200.0	5.19	1.0	0.65	0.75	1.0

(b) TLCDs' variable parameters in experiments

Mass ratio μ	Vertical area A_v(m^2)	Horizontal area A_h(m^2)
0.1	6.76×10^{-4}	6.76×10^{-4}
0.2	1.37×10^{-3}	1.37×10^{-3}
0.3	2.03×10^{-3}	2.03×10^{-3}

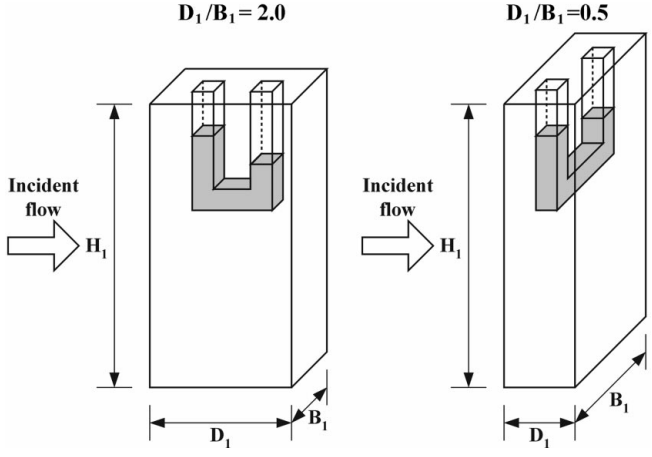

Fig. 5 Directions of model installation

the structural vibration in the along-wind and the across-wind directions. The sampling frequency was 500.0 Hz and the time duration was 65.5 sec in this study.

3.2. Wind load

Spires and roughness elements were provided to generate a boundary layer flow in the wind tunnel. Fig. 6(a) shows the profiles of the mean wind velocity and the turbulent intensity measured

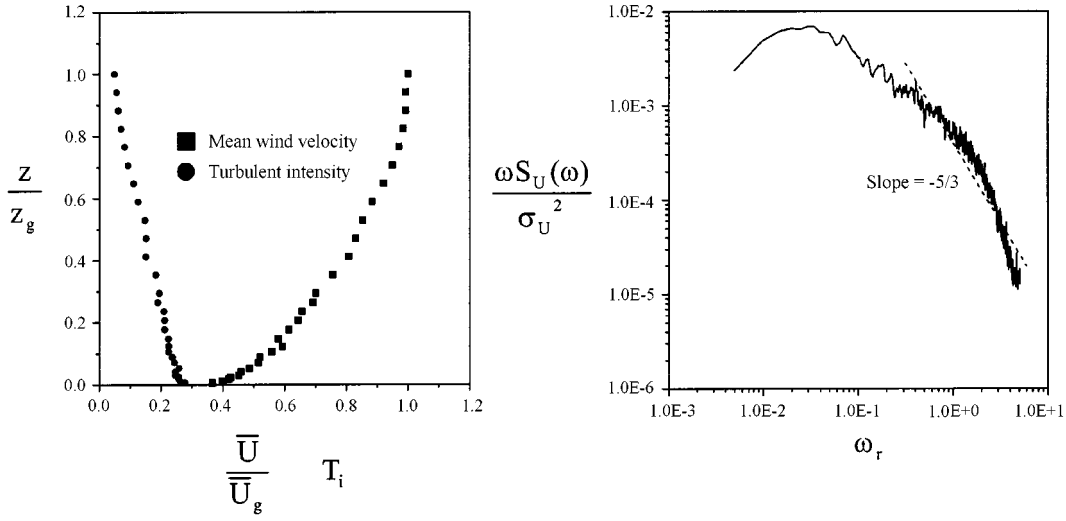

(a) Profiles of mean wind velocity and turbulent intensity (b) Longitudinal wind velocity spectrum

Fig. 6 Wind field in experiments

by a hot-wire anemometer, where z and $\overline{U}$ are defined as the height and the mean wind velocity, respectively. Furthermore, subscript g denotes the gradient value of the corresponding parameter. A suburban area ($\alpha = 0.25$) is simulated with type B terrain. Consequently, the roughness coefficient K_0 is 0.01 (Mehta and Marshall 1998). Moreover, the turbulent intensity T_i is 27.8% near the ground, but 4.8% at the top of wind tunnel. Mehta and Marshall (1998) have proposed that the equivalent height of a flexible structure is $0.6\,H_1$, where H_1 is defined as the height of the building. In this research, the nominal value of T_i can be determined in this position. Fig. 6(a) indicates that T_i of the corresponding height ($z/z_g = 0.26$) is 19.0%. The longitudinal wind velocity spectrum $S_U(\omega)$ for the reduced wind velocity $\overline{U}_r = 22.6$ is illustrated in Fig. 6(b), where ω_r is the reduced circular frequency and σ_U is the RMS wind velocity, separately. It shows that the slope is -5/3. This result coincides with Kolmogorov's research (1941).

The wind load coefficients are presented in Table 3. $\overline{C}_{s_f}$ and $\overline{C}_{y_m}$ are defined as the mean side force and the mean yawing moment coefficients, while $\overline{C}_{r_m}$ and $\overline{C}_{p_m}$ represent the mean rolling moment and the mean pitching moment coefficients. Furthermore, the superscript $'$ denotes the RMS value of the corresponding coefficient. Table 3 indicates that all wind load coefficients for $D_1/B_1 = 0.5$ are higher than $D_1/B_1 = 2.0$, except for C'_{y_m}. Since the shape of the model is symmetric

Table 3 Wind load coefficients in experiments

Wind load coefficients	Mean values		RMS values				
	Drag	Pitching moment	Drag	Side force	Rolling moment	Pitching moment	Yawing moment
	$\overline{C}_d$	$\overline{C}_{p_m}$	C'_d	C'_{s_f}	C'_{r_m}	C'_{p_m}	C'_{y_m}
$D_1/B_1 = 2.0$	1.08	0.23	0.15	0.12	0.07	0.09	0.04
$D_1/B_1 = 0.5$	1.20	0.31	0.20	0.33	0.17	0.13	0.01

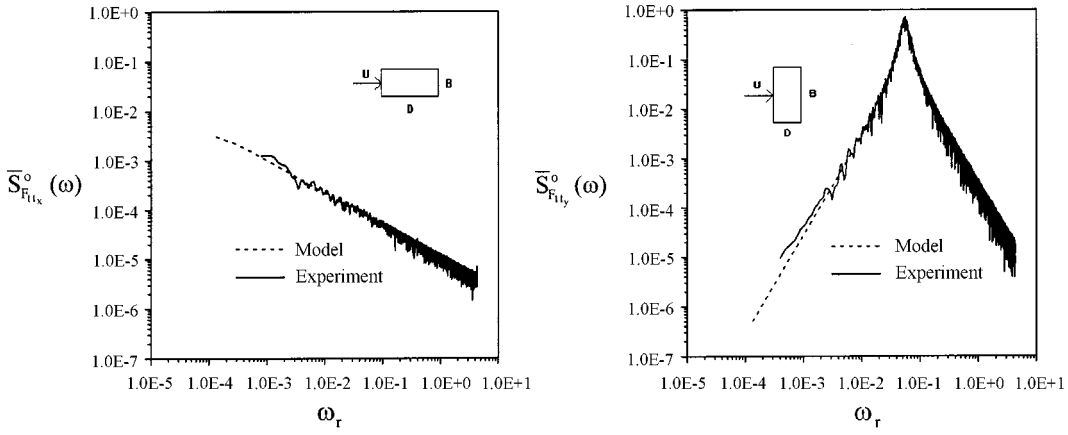

(a) Along-wind direction (b) Across-wind direction

Fig. 7 Dimensionless generalized wind load spectra

and its windward face is orthogonal to the incident flow, then $\bar{C}_{s_f}$, $\bar{C}_{r_m}$ and $\bar{C}_{y_m}$ approximate 0 in this study. These experimental results are consistent with previous studies (Matsumoto 1986, Kanda and Choi 1992 and Hayashida, *et al*. 1992).

The dimensionless generalized along-wind load spectrum $\bar{S}^o_{F_{11_x}}(\omega)$ $(\equiv \omega \bar{S}_{F_{11_x}}(\omega)/(0.5\rho_a \bar{U}_1^2 \sqrt{B_1 D_1 H_1})^2)$ and the dimensionless generalized across-wind load spectrum $\bar{S}^o_{F_{11_y}}(\omega)$ $(\equiv \omega \bar{S}_{F_{11_y}}(\omega)/(0.5\rho_a \bar{U}_1^2 \sqrt{B_1 D_1 H_1})^2)$ for $\bar{U}_r$ = 22.6 are illustrated in Fig. 7(a) and Fig. 7(b), respectively. Fig. 7(a) shows that the experimental values $(D_1/B_1 = 2.0)$ conform to Eq. (10a). The amplitude of $\bar{S}^o_{F_{11_x}}(\omega)$ falls almost within the low-frequency region. Fig. 7(b) implies that the experimental data $(D_1/B_1 = 0.5)$ coincide with Eq. (10b). The lock-in phenomenon will appear if the corresponding frequency of the sharp peak in $\bar{S}^o_{F_{11_y}}(\omega)$ is close to the natural circular frequency of the structure ω_1. The across-wind response of a building will become severer in this condition. As indicated earlier, these experimental results agree substantially with Davenport's along-wind and Ohkuma and Kanaya's across-wind load spectra. Therefore, these two spectra can properly be utilized to calculate the structural response. Table 4 presents the coefficients of the wind load spectra used in this experimental investigation.

Table 4 Coefficients of wind load spectra in experiments

Along-wind direction $(D_1/B_1 = 2.0)$	Power law exponent α	0.25
	Roughness coefficient K_0	0.01
	Air density ρ_a(kg / m^3)	1.2
	Mean drag coefficient $\bar{C}_d$	1.08
	Decay coefficient C_x	8.0
Across-wind direction $(D_1/B_1 = 0.5)$	Strouhal number S_t	0.08
	Bandwidth coefficient B_w	0.12
	Decay coefficient C_y	6.67

3.3. Structural response

The along-wind oscillation without the aerodynamic effects was considered in this research. Fig. 8(a) and Fig. 8(b) show the variations in the dimensionless RMS displacement $\sigma^o_{X_{1x}}$ ($\equiv \sigma_{X_{1x}} / \sqrt{B_1 D_1}$) and the dimensionless RMS acceleration $\sigma^o_{\ddot{X}_{1x}}$ ($\equiv 4\pi^2 \sigma_{\ddot{X}_{1x}} / \omega_1^2 \sqrt{B_1 D_1}$) over $\overline{U}_r$ in the along-wind direction. These two diagrams illustrate that the experimental values conform to the analytical model shown in Fig. 3. Consequently, this model may be used to correctly calculate the along-wind vibration. Both $\sigma^o_{X_{1x}}$ and $\sigma^o_{\ddot{X}_{1x}}$ increase with an increase in $\overline{U}_r$. Furthermore, the TLCD is more effective in suppressing both $\sigma^o_{X_{1x}}$ and $\sigma^o_{\ddot{X}_{1x}}$ for higher values of $\overline{U}_r$. These diagrams also indicate that both $\sigma^o_{X_{1x}}$ and $\sigma^o_{\ddot{X}_{1x}}$ decrease when μ increases. Therefore, the TLCD with a greater mass is more advantageous in controlling the along-wind response, being more useful for reducing $\sigma^o_{\ddot{X}_{1x}}$ than $\sigma^o_{X_{1x}}$. These results are consistent with the analytical studies of Xu, *et al*. (1992b) and Sun, *et al*. (1993).

The aerodynamic response in the across-wind direction was measured by the instrument, as shown in Fig. 4(b). Based on the across-wind load spectrum measured by the high-frequency force balance shown in Fig. 4(a), the structural oscillation can be evaluated without the aerodynamic effects. The aerodynamic damping ratio ξ_a can then be obtained (Cermak and Isyumov 1999). According to the wind tunnel experiments, $C_1^* = -2.5$ and $C_2^* = -0.1$ are determined and used to calculate ξ_a in Eq. (5f). Fig. 9 illustrates the relationship between ξ_a and $\overline{U}_r$. The predictive and experimental values agree well. This diagram reveals that negative values of ξ_a are pronounced for square-sectional buildings. This result coincides with Vickery's experimental research (1995). Fig. 10(a) and Fig. 10(b) present variations in the dimensionless RMS displacement $\sigma^o_{X_{1y}}$ ($\equiv \sigma_{X_{1y}} / \sqrt{B_1 D_1}$) and the dimensionless RMS acceleration $\sigma^o_{\ddot{X}_{1y}}$ ($\equiv 4\pi^2 \sigma_{\ddot{X}_{1y}} / \omega_1^2 \sqrt{B_1 D_1}$) over $\overline{U}_r$, whether ξ_a is separately considered in the across-wind direction. These two diagrams indicate that the experimental values support the analytical model in Fig. 3. Furthermore, this model is also in substantial agreement with the experimental studies (Kwok 1982, Kareem 1984, Matsumoto 1986 and Kawai 1992). It may therefore evaluate the aerodynamic response accurately. Both $\sigma^o_{X_{1y}}$ and $\sigma^o_{\ddot{X}_{1y}}$ reach a maximum when the lock-in phenomenon occurs. In this condition, the reduced resonant wind velocity $\overline{U}_r^L$ is 17.4. The TLCD is obviously more effective in suppressing both $\sigma^o_{X_{1y}}$ and $\sigma^o_{\ddot{X}_{1y}}$ in $\overline{U}_r^L$. Since a negative value ξ_a for reducing the damping ratio of the structure ξ_1, then both $\sigma^o_{X_{1y}}$ and $\sigma^o_{\ddot{X}_{1y}}$ are underestimated without ξ_a, especially in the region neighboring $\overline{U}_r^L$. Consequently, the aerodynamic effects are significant when the across-wind oscillation is considered. Moreover, the predictive model properly reflects aerodynamic effect characteristics in this investigation. Fig. 10(a) and Fig. 10(b) also demonstrate that both $\sigma^o_{X_{1y}}$ and $\sigma^o_{\ddot{X}_{1y}}$ decrease as μ increases. As a result, the TLCD with a greater mass is more useful in controlling the across-wind vibration. In addition, the TLCD is more advantageous for reducing $\sigma^o_{\ddot{X}_{1y}}$ than $\sigma^o_{X_{1y}}$. These results are consistent with the analytical studies of Xu, *et al*. (1992a).

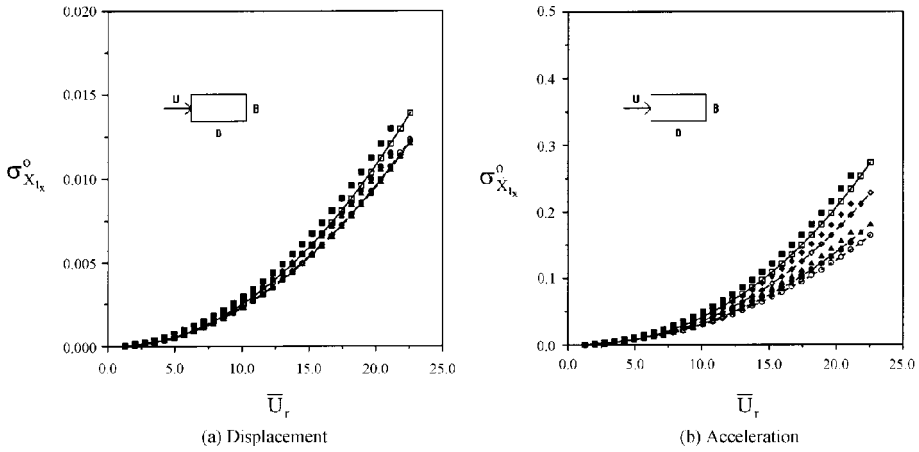

Fig. 8 Variations in dimensionless RMS structural oscillation over reduced wind velocity in along-wind direction

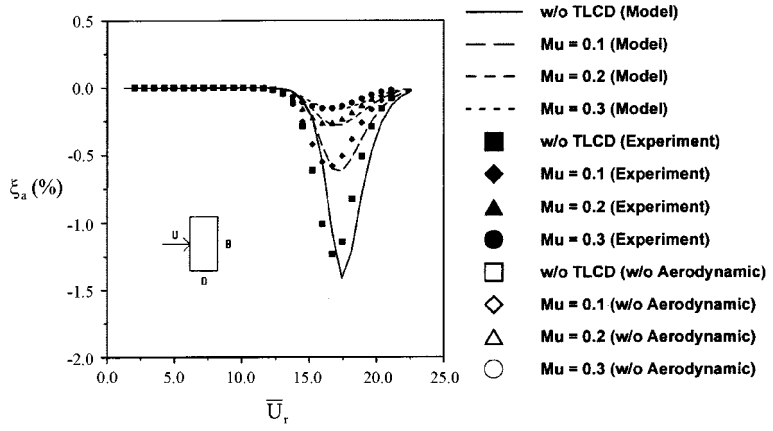

Fig. 9 Relationship between aerodynamic damping ratio and reduced wind velocity

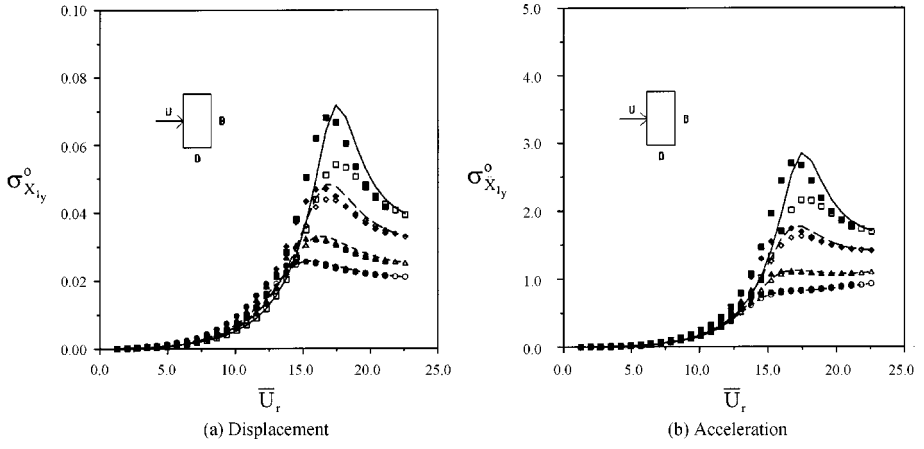

Fig. 10 Variations in dimensionless RMS structural oscillation over reduced wind velocity in across-wind direction

4. Parametric studies

A forty-story building with a TLCD in an urban area belongs to type A terrain (Mehta and Marshall 1998). Table 5 presents the coefficients of the wind load spectra used in the parametric studies. The breadth (B_1), depth (D_1) and height (H_1) of the building were 40 m, 40 m and 160 m, respectively (see Fig. 2). The aspect ratio A_r was 4.0. As indicated earlier, the mode shape of the vibration system was assumed to be linear. Furthermore, a building with a TLCD can be simulated as a two-degree-of-freedom oscillation system. Generalized parameters for the first mode of the building in Table 6 were utilized to evaluate the structural response. The tuning ratio δ, the mass ratio μ, the dimensional ratio λ, the orifice opening ratio κ and the area ratio χ are the five significant TLCD parameters, which act to suppress the wind-induced oscillation. In order to

Table 5 Coefficients of wind load spectra in parametric studies

Along-wind direction	Power law exponent α	0.36
	Roughness coefficient K_0	0.025
	Air density ρ_a(kg/m^3)	1.2
	Mean drag coefficient $\bar{C}_d$	1.3
	Decay coefficient C_x	8.0
Across-wind direction	Strouhal number S_t	0.08
	Bandwidth coefficient B_w	0.18
	Decay coefficient C_y	6.67

Table 6 Generalized parameters for the first mode of the building in parametric studies

Mass	Damping coefficient	Stiffness	Natural circular frequency	Damping ratio
M_1(kg)	C_1(N-sec/m)	K_1(N/m)	ω_1(rad/sec)	ξ_1
1.76×10^7	1.15×10^6	4.73×10^7	1.64	0.02

Table 7 (a) Invariable parameters in parametric studies

Tuning ratio	Mass ratio	Dimensional ratio	Orifice opening ratio	Area ratio
δ	μ	λ	κ	χ
1.0	0.15	0.8	0.75	1.0

(b) Variable parameters in parametric studies

Tuning ratio	Mass ratio	Dimensional ratio	Orifice opening ratio	Area ratio
δ	μ	λ	κ	χ
0.33	0.03	0.6	0	0.7
0.5	0.06	0.7	0.25	0.85
1.0	0.09	0.8	0.50	1.0
2.0	0.12	0.9	0.75	1.15
3.0	0.15	1.0	1.0	1.3

independently investigate the effectiveness of these parameters, a series of parametric studies based on the analytical model in Fig. 3 were carried out, varying a single parameter at a time. The invariable and the variable parameters are summarized in Table 7(a) and Table 7(b), respectively.

Parametric studies were practiced when the lock-in phenomenon occurred. The reduced resonant wind velocity $\overline{U}_r^L$ was 13.8 in this condition. The variations in the oscillatory response ratio R_r (defined as the proportion of the controlled to the uncontrolled RMS vibration of a building) over δ, μ, λ, κ and χ are individually presented in Fig. 11(a) through Fig. 11(e). Fig. 11(a) implies that the TLCD with $\delta = 1.0$ gives the maximum R_r reduction, which conforms to the research of Balendra, *et al.* (1995). Since the movement of the horizontal liquid can increase the inertia force in suppressing oscillation, R_r decreases when μ increases, as shown in Fig. 11(b). As a result, the TLCD with a greater mass is more useful in controlling the structural response. This is consistent with the experimental studies mentioned in chapter three. In addition, the TLCD with a greater λ value more effectively reduce R_r, as illustrated in Fig. 11(c), which is also due to the added inertia force. Fig. 11(d) indicates that R_r decreases as κ increases. This reduction is correlated with the damping effect caused by an orifice. Because the restoring load induced by gravity on the liquid can dissipate the vibration energy, the TLCD with a greater χ value more effectively suppresses R_r, as shown in Fig. 11(e). These five diagrams also indicate that the TLCD is more advantageous for reducing the across-wind oscillation than the along-wind vibration. When across-wind aerodynamic

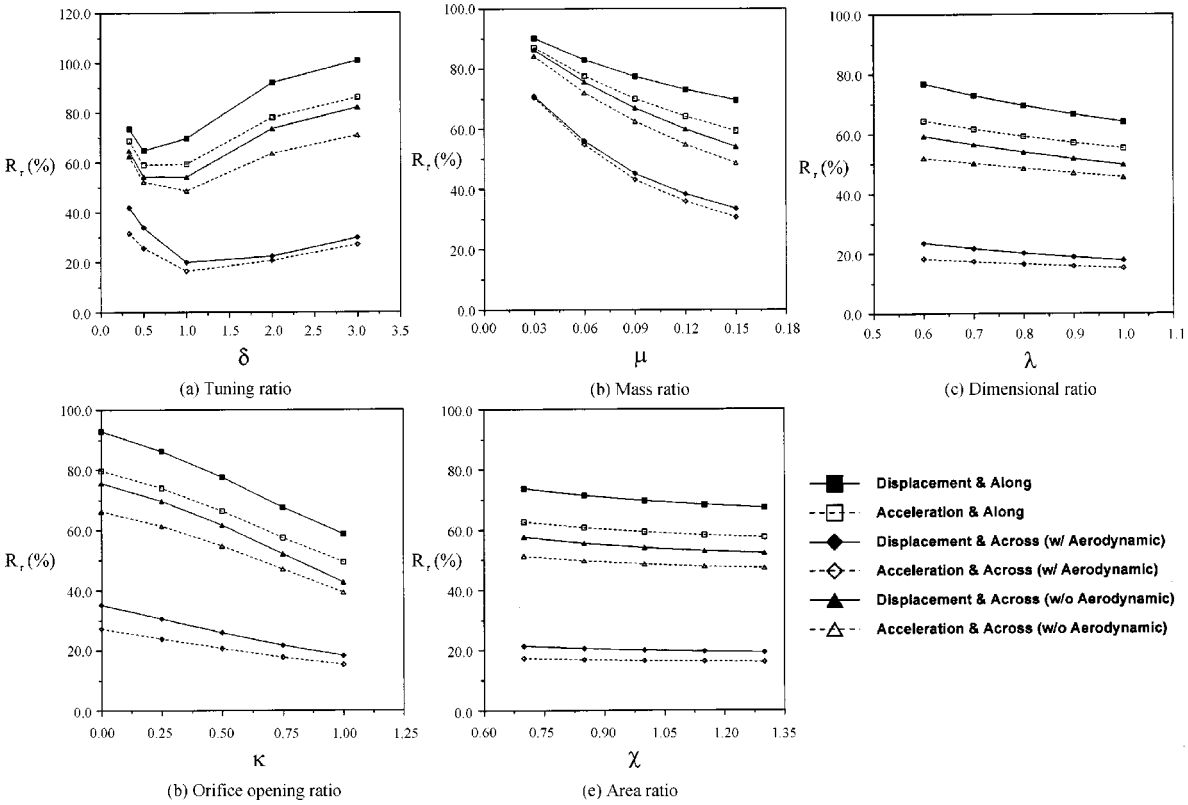

Fig. 11 Variations in oscillatory response ratio over TLCD's parameters

effects are considered, the TLCD more effectively controls the aerodynamic response, reducing the acceleration more than the displacement in biaxial directions. These results from parametric studies are in substantial agreement with previous studies (Samali, *et al*. 1992, Balendra, *et al*. 1995, Won, *et al*. 1997 and Gao and Kwok 1997). Consequently, TLCDs are effective devices for suppressing the wind-induced vibration in buildings.

5. Conclusions

In this research, wind tunnel experiments were carried out to study the wind-induced vibration in a building with a TLCD. A predictive model of the aerodynamic response in the across-wind direction was created, leading to the development of a computing procedure for the analytical modeling of the structural oscillation in a building with a TLCD under the wind load. Parametric studies were also used to calculate the effectiveness of the TLCD in controlling wind-induced vibration in a structure. Eventually, several conclusions were generated based on this investigation.

1. The aerodynamic damping ratio predictive model is a function of Scruton number, the turbulent intensity, the dimensionless RMS displacement of the structure in the across-wind direction, the aspect ratio, the reduced wind velocity and the reduced resonant wind velocity. Two undetermined coefficients of this model were computed experimentally. As a result, this model does reflect the aerodynamic effect characteristics. It can thus be used to calculate the aerodynamic damping ratio, so that the aerodynamic response of a building may be accurately evaluated in the across-wind direction.
2. A computing procedure has been generated for the analytical modeling of the wind-induced vibration in a building with a TLCD. It agrees substantially with the experimental data. Therefore, this model may be used to correctly calculate both the along-wind and the across-wind response.
3. Results from this investigation show that the TLCD is more useful in suppressing the along-wind response for higher wind velocity values. It is also more effective in controlling the across-wind oscillation when the lock-in phenomenon occurs. Moreover, the TLCD is more advantageous for reducing the across-wind vibration than the along-wind oscillation. When the across-wind aerodynamic effects are considered, the TLCD is more effective in controlling the aerodynamic response. They are also more useful in reducing the acceleration than the displacement in biaxial directions. As s result, TLCDs are effective devices for suppressing the structural vibration under the wind load.
4. Based on results from parametric studies, the TLCD has more benefit for reducing the wind-induced oscillation in a building, when the tuning ratio is equal to 1.0. It is also more effective when greater mass ratio, dimensional ratio, orifice opening ratio and area ratio values are used.
5. This study may help engineers to more correctly predict the aerodynamic response of high-rise buildings as well as select the most appropriate TLCDs for reducing the structural oscillation under the wind load. This could improve the understanding of wind-structure interactions and wind resistant designs for high-rise buildings.

Acknowledgements

The authors gratefully acknowledge the support provided by National Science Council (NSC) of Taiwan, R.O.C. under the project NSC 89-2211-E-008-029.

References

Balendra, T., Wang, C.M. and Cheong, H.F. (1995), "Effectiveness of tuned liquid column dampers for vibration control of towers", *Engineering Structures*, **17**(9), 668-675.

Basu, R.I. and Vickery, B.J. (1983), "Across-wind vibrations of structures of circular cross-section. Part II. Development of a mathematical model for full-scale application", *J. Wind Eng. Ind. Aerod.*, **12**, 75-97.

Cermak, J.E. and Isyumov, N. (1999). *Wind tunnel studies of buildings and structures*, ASCE Press, Virginia, U.S.A.

Cheng, C.M., Lo, H.Y. and Lu, P.C. (1999), "Acrosswind responses of square shaped high-rise buildings with eccentricities", *Proceedings of 10th International Conference on Wind Engineering*, Copenhagen, Denmark, 631-636.

Davenport, A.G. (1976). *Vibration of structures induced by wind*, *Shock and Vibration Handbook*, McGraw-Hill, Inc., New York, U.S.A.

Gao, H. and Kwok, K.C.S. (1997), "Optimization of tuned liquid column dampers", *Engineering Structures*, **19**(6), 476-486.

Hayashida, H., Mataki, Y. and Iwasa, Y. (1992), "Aerodynamic damping effects of tall building for a vortex induced vibration", *J. Wind Eng. Ind. Aerod.*, **41-44**, 1973-1983.

Iwan, W.D. and Yang, I.M. (1972), "Application of statistical linearization technique to nonlinear multidegree-of-freedom systems", *Journal of Applied Mechanics, ASME*, **39**, 545-550.

Kanda, J. and Choi, H. (1992), "Correlating dynamic wind force components on 3-D cylinders", *J. Wind Eng. Ind. Aerod.*, **41-44**, 785-796.

Kareem, A. (1984), "Model for predicting the acrosswind response of buildings", *Engineering Structures*, **6**, 136-141.

Kareem, A. (1992), "Dynamics response of high-rise buildings to stochastic wind loads", *J. Wind Eng. Ind. Aerod.*, **41-44**, 1101-1112.

Kawai, H. (1992), "Vortex induced vibration of tall buildings", *J. Wind Eng. Ind. Aerod.*, **41-44**, 117-128.

Kolmogorov, A.N. (1941), "The local structure of turbulence in incompressible viscous fluid for very large Reynolds numbers", *Dokl. Akad. Nauk, SSSR*, **4**, 299-319.

Kwok, K.C.S. (1982), "Cross-wind response of tall buildings", *Engineering Structures*, **4**, 256-262.

Matsumoto, T. (1986), "On the across-wind oscillation of tall buildings", *J. Wind Eng. Ind. Aerod.*, **24**, 69-85.

Mehta, K.C. and Marshall R.D. (1998), *Guide to the use of the wind load provisions of ASCE 7-95*, ASCE Press, Virginia, U.S.A.

Ohkuma, T. and Kanaya, A. (1978), "On the correlation between the shape of rectangular cylinders and characteristics of fluctuating lifts on them", *Proceedings of 5th Symposium on Wind Effects on Structures*, Tokyo, Japan, 147-154 (in Japanese).

Sakai, F., Takaeda, S. and Tamaki, T. (1989), "Tuned liquid column damper-new type device for suppression of building vibration", *Proceedings of 1st International Conference on High-Rise Buildings*, Nanjing, China, 926-931.

Samali, B., Kwok, K.C.S., Young, G. and Xu, Y.L. (1992), "Effectiveness of optimized tuned liquid column dampers in controlling vibration of tall buildings subject to strong ground motions", *Proceedings of 2nd International Conference on High-Rise Buildings*, Nanjing, China, 402-407.

Sun, K., Cheong, H.F. and Balendra, T. (1993), "Effect of liquid dampers on along-wind response of structures", *Proceedings of 3rd Asia-Pacific Symposium on Wind Engineering*, Hong Kong, 835-840.

Vickery, B.J. (1981), "Across-wind buffeting in a group of four in-line model chimneys", *J. Wind Eng. Ind. Aerod.*, **8**, 177-193.

Vickery, B.J. and Basu, R.I. (1983), "Across-wind vibrations of structures of circular cross-section. Part I. Development of a mathematical model for two-dimensional conditions", *J. Wind Eng. Ind. Aerod.*, **12**, 49-73.

Vickery, B.J. and Basu, R.I. (1984), "The response of reinforced concrete chimneys to vortex shedding", *Engineering Structures*, **6**, 324-333.

Vickery, B.J. (1995), "The response of chimneys and tower-like structures to wind loading", *State of the Art Volume, 9th International Conference on Wind Engineering*, New Delhi, India, 205-233.

Won, A.Y.J., Pires, J.A., and Haroun, M.A. (1997), "Performance assessment of tuned liquid column dampers

under random seismic loading", *International Journal of Non-Linear Mechanics*, **32**(4), 745-758.
Xu, Y.L., Kwok, K.C.S. and Samali, B. (1992a), "The effect of tuned mass dampers and liquid dampers on cross-wind response of tall/slender structures", *J. Wind Eng. Ind. Aerod.*, **40**, 33-54.
Xu, Y.L., Samali, B. and Kwok, K.C.S. (1992b), "Control of along-wind response of structures by mass and liquid dampers", *J. Eng. Mechanics*, ASCE, **118**(1), 20-39.

CC